Self-rotation and synchronization in exciton-polariton condensates

Hiroki Saito[1] and Rina Kanamoto[2]

[1]*Department of Engineering Science, University of Electro-Communications, Tokyo 182-8585, Japan*
[2]*Department of Physics, Meiji University, Kawasaki, Kanagawa 214-8571, Japan*

(Received 24 June 2016; revised manuscript received 30 August 2016; published 18 October 2016)

Self-rotation occurs in an exciton-polariton condensate in a two-dimensional semiconductor microcavity pumped by a nonresonant Gaussian laser beam. A wave packet of the condensate spontaneously rotates around the center of the pumped region at a constant frequency breaking the rotation symmetry of the system. When two self-rotating condensates are created with an appropriate distance, synchronization occurs between the dynamics of the self-rotating condensates.

I. INTRODUCTION

Self-oscillations are ubiquitous phenomena that occur in nature, ranging from whistles and heartbeats to pulsating variable stars [1]. Self-oscillation is induced by some instability and maintained by the oscillation itself, i.e., external energy is synchronously taken into the system, which balances with dissipation, and results in the stable limit cycle in the phase space. When two or more self-oscillators are coupled with each other, synchronization can occur between their oscillations, as Huygens observed in pendulum clocks [2].

Self-oscillation can be observed in open quantum systems with nonlinearity, in which energy is replenished from and dissipated into their environments. Laser and Josephson oscillations may be regarded as self-oscillations in quantum systems. Self-oscillations have also been observed in optomechanical systems [3,4] and in a resonator driven by a superconducting single-electron transistor [5]. Here, we focus on exciton-polariton condensates in a planar microcavity [6,7] as an open quantum system to investigate the self-oscillation. Exciton-polaritons excited by external laser beams have a lifetime of picoseconds, which is of the same order as the characteristic time scale of polariton dynamics. Therefore, the exciton-polariton condensate is a nonequilibrium open system. Various experiments have been performed on this system, such as observations of Bose-Einstein condensation [8], quantized vortices [9,10], quantum hydrodynamics [11–14], and a chaotic non-Hermitian billiard [15]. Self-oscillations and synchronization in exciton-polariton condensates have been predicted in Refs. [16–23], and the phase locking of condensates has been reported in Refs. [24,25]. The Bénard–von Kármán vortex street in an exciton-polariton superfluid [26] can also be regarded as self-oscillation.

In this paper, we show that a wave packet of an exciton-polariton condensate that is nonresonantly pumped by a Gaussian laser beam rotates spontaneously around the center of the pumped region. This self-rotation is a consequence of spontaneous breaking of the rotation and clockwise-counterclockwise symmetries, and the system acquires an angular momentum. We also show that when two self-rotating condensates are excited by two Gaussian laser beams with an appropriate distance between them, the rotating dynamics are synchronized, even when the individual rotation frequency is different.

This paper is organized as follows. The problem is formulated and the properties of the uniform system are reviewed in Sec. II. The self-rotation of the condensate is investigated in Sec. III. The synchronization of two self-rotating condensates is demonstrated in Sec. IV. Conclusions and discussion are provided in Sec. V.

II. MODULATIONAL INSTABILITY IN A HOMOGENEOUS SYSTEM

First, we formulate the problem and give a brief review of the modulational instability in a homogeneous system. The dynamics of an exciton-polariton condensate with an effective mass m is modeled by the nonlinear Schrödinger equation given by [27]

$$i\hbar \frac{\partial \psi}{\partial t} = -\frac{\hbar^2}{2m} \nabla^2 \psi + \frac{i\hbar}{2}(R n_R - \gamma_c)\psi + g_c |\psi|^2 \psi + g_R n_R \psi, \tag{1}$$

where $\psi(\mathbf{r},t)$ is the macroscopic wave function of the exciton-polariton condensate and $n_R(\mathbf{r},t)$ represents the polariton density of the reservoir, which obeys

$$\frac{\partial n_R}{\partial t} = P - \gamma_R n_R - R n_R |\psi|^2. \tag{2}$$

The external laser pump P creates polaritons with much larger energy than that of the condensate polaritons in the lower branch. The pumped polaritons then relax and form the reservoir n_R, which feeds polaritons to the condensate with a rate R. In this section, we consider a homogeneous pump with a constant P. The loss rates of the condensate and reservoir polaritons are γ_c and γ_R, respectively. In Eq. (1), the condensate polaritons interact with each other through the nonlinear term with a coefficient g_c, and the interaction between the condensate and reservoir polaritons is described by the term with g_R.

In a homogeneous system, the polariton densities in the steady state above the condensation threshold are given by $|\psi_0|^2 = (P - P_{\text{th}})/\gamma_c$ and $n_{R0} = \gamma_c/R$, where $P_{\text{th}} = \gamma_c \gamma_R/R$. This homogeneous solution is modulationally unstable [20,27–29] for $P_{\text{th}} < P < \frac{\gamma_c g_R}{\gamma_R g_c} P_{\text{th}}$ when $\frac{\gamma_c g_R}{\gamma_R g_c} > 1$. The instability can be explained by the effective attractive interaction in the condensate [28]. Figure 1(a) shows the dynamics of the density profiles under modulational instability, where the initial state is $\psi = \psi_0$ and $n_R = n_{R0}$ with a small random noise, which is a random number set on each numerical mesh. In this and the following numerical simulations, the
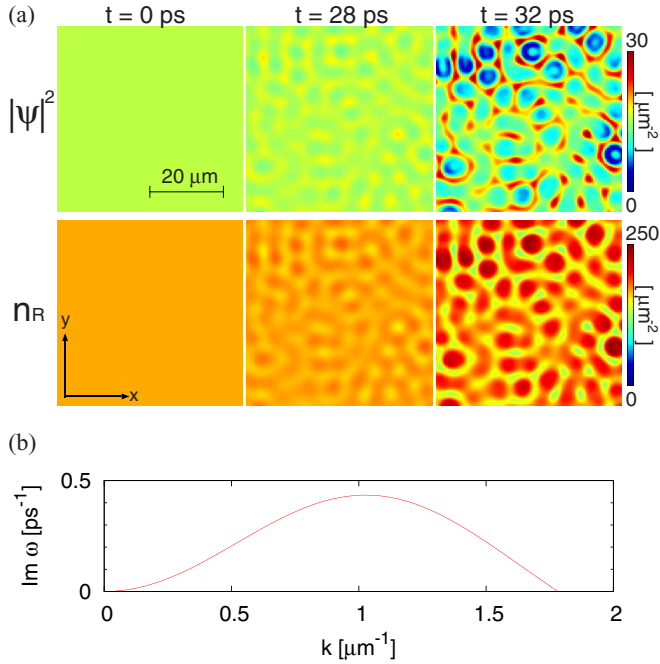
FIG. 1. Modulational instability in the uniform system with $\gamma_c^{-1} = 0.15$ ps, $\gamma_R^{-1} = 3$ ps, $g_c = 6 \times 10^{-3}$ meV μm^2, $g_R = 2g_c$, $R = 0.04$ ps^{-1} μm^2, $P = 160$ ps^{-1} μm$^{-2} \simeq 2.9P_{th}$, and $m = 5 \times 10^{-5}$ electron mass. (a) Time evolution of the condensate and reservoir density profiles, $|\psi|^2$ and n_R, where the initial state is the homogeneous stationary state. (b) Positive imaginary part of the Bogoliubov spectrum.

pseudospectral method with the fourth-order Runge-Kutta scheme is employed. The unstable wavelengths can be obtained from the Bogoliubov analysis. Substituting $\psi(\mathbf{r},t) = [\psi_0 + u_k e^{i\mathbf{k}\cdot\mathbf{r}-i\omega t} + v_k^* e^{-i\mathbf{k}\cdot\mathbf{r}-i\omega^* t}]e^{-i\mu t/\hbar}$ and $n_R(\mathbf{r},t) = n_{R0} + \mathrm{Re}(n_k e^{i\mathbf{k}\cdot\mathbf{r}-i\omega t})$ with $\mu = g_c|\psi_0|^2 + g_R n_{R0}$ into Eqs. (1) and (2) and diagonalizing the 3×3 matrix, we obtain the Bogoliubov spectrum $\omega(k)$ and mode coefficients u_k, v_k, and n_k. When the imaginary part of $\omega(k)$ is positive, the mode with the wave number k is unstable. Figure 1(b) shows the imaginary part of $\omega(k)$. The most unstable wavelength is $\lambda \simeq 2\pi$ μm, which agrees with the pattern in Fig. 1(a).

III. SPONTANEOUS ROTATION WITH A GAUSSIAN PUMP

We consider a situation in which exciton-polaritons are pumped by a Gaussian laser beam. The pump profile is given by

$$P(\mathbf{r}) = P_0 e^{-r^2/\rho^2}, \quad (3)$$

where P_0 is the peak intensity and ρ is the $1/e$ width of the beam. When the pump width ρ is much larger than the unstable wavelengths of a homogeneous system pumped by $P = P_0$, the central region of the pump is sufficiently wide for modulational instability and pattern formation. On the other hand, when ρ is much smaller than the unstable wavelengths, no modulational instability occurs in the Gaussian-shaped condensate. An interesting situation is expected for ρ comparable to the unstable wavelength. Self-oscillations have been observed in a one-dimensional system in this regime [20].
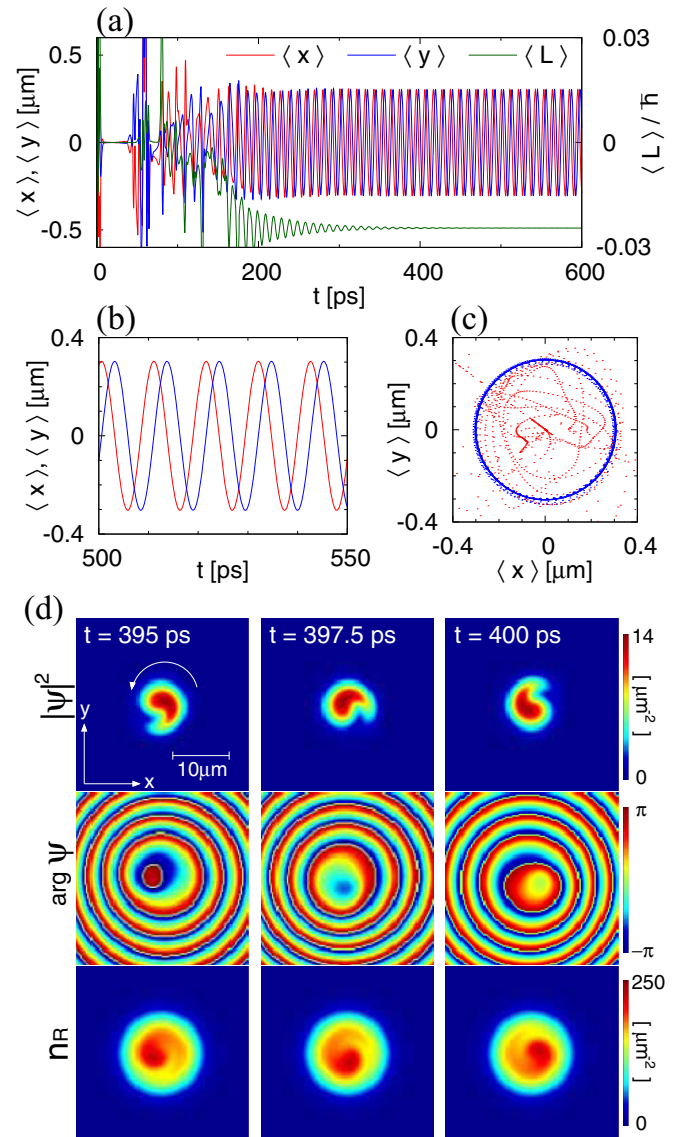

FIG. 2. Time evolution of the system pumped by a Gaussian laser beam with $P_0 = 160$ ps^{-1} μm^{-2} and $\rho = 5$ μm. The other parameters are $\gamma_c^{-1} = 0.15$ ps, $\gamma_R^{-1} = 3$ ps, $g_c = 6 \times 10^{-3}$ meV μm^2, $g_R = 2g_c$, and $R = 0.04$ ps^{-1} μm^2. (a) Time evolution of the center-of-mass (c.m.) position ($\langle x \rangle, \langle y \rangle$) and the angular momentum $\langle L \rangle$ of the condensate. (b) Magnification of (a). (c) Trajectory of ($\langle x \rangle, \langle y \rangle$), where the red and blue points are $t < 200$ ps and $t > 200$ ps, respectively. The points are plotted every 0.17 ps. (d) Snapshots of the density and phase profiles, $|\psi|^2$, $\arg\psi$, and n_R. The white arrow indicates the direction of rotation for the c.m. position. See the Supplemental Material for a movie of the dynamics [30].

Figure 2 shows the dynamics of the system pumped by a Gaussian laser beam with $\rho = 5$ μm, where the initial state is $\psi = n_R = 0$ plus a small random noise. Figures 2(a)–2(c) show the time evolution of the center-of-mass (c.m.) position,

$$\langle \mathbf{r} \rangle = \frac{\int \mathbf{r}|\psi|^2 d\mathbf{r}}{\int |\psi|^2 d\mathbf{r}}, \quad (4)$$

and the angular momentum per particle,

$$\langle L \rangle = \frac{-i\hbar \int \psi^*(x\partial_y - y\partial_x)\psi \, d\boldsymbol{r}}{\int |\psi|^2 d\boldsymbol{r}}, \qquad (5)$$

of the condensate. After $t \sim 200$ ps, the c.m. motion becomes periodic and the angular momentum converges to a constant value. The trajectory of $\langle \boldsymbol{r} \rangle$ is entrained into a circle and rotates along the circle at a constant angular frequency. This circular trajectory is robust against external perturbation. We have confirmed that the trajectory always returns to the circle after the regular dynamics are disturbed by a temporal external potential. We have also confirmed that the circular trajectory is always realized irrespective of the random seed to produce the initial noise. These facts imply that the circular trajectory is the stable limit cycle and the rotating state is the steady state reached from any initial states.

Figure 2(d) shows the time evolution of the density and phase profiles after the steady rotating state is reached. A tadpole-shaped condensate wave packet rotates around the center counterclockwise. It is interesting to note that the angular momentum $\langle L \rangle$ is negative, whereas the tadpole-shaped wave packet rotates counterclockwise. This seeming contradiction arises from the superflow in the condensate. Figure 2(d) shows $\arg\psi$, which indicates that the superfluid flows out from the point near the head of the tadpole, and results in superflow from the head to the tail of the tadpole. This is because the condensate is fed from the reservoir mainly at the head of the tadpole, because the density of the reservoir is large ahead of the tadpole. As a result, the tadpole grows ahead, while the tail is always shrunk by the dissipation. This is the reason why the directions of the tadpole rotation and the angular momentum are opposite. For initial noises with different random seeds, $\langle L \rangle > 0$ and $\langle L \rangle < 0$ occurs with the same probability due to the chiral symmetry of the system.

The pump with a Gaussian beam thus induces the rotation dynamics, which can be regarded as self-rotation, because the rotation symmetry of the system is spontaneously broken and the stable rotation persists without any external rotating force. The rotation is driven by the interplay between the condensate and reservoir; the tadpole-shaped condensate grows ahead due to the density gradient in the reservoir, while the high density region of the reservoir chases the tail of the tadpole where the supply to the condensate is small.

Figure 3 shows the parameter dependence of the period of the self-rotation. The self-rotation frequency increases with P_0, R, and g_R, and decreases as γ_c, γ_R, and g_c increase.

Experimentally, there always exist imperfections in a sample of the semiconductor microcavity, which produces random potential for polaritons. We have performed numerical simulations including random potential with a typical energy of ~ 0.1 meV and spatial scale of $\sim 10\mu$m, and confirmed that the self-rotation as shown in Fig. 2 occurs even in the presence of the disorder potential (see the Supplemental Material for a movie of the dynamics [30]).

One may think that the self-rotation in Fig. 2 is triggered by the unrealistic oscillation between the condensate and reservoir in the early stage of the dynamics. We have confirmed that the self-rotation occurs even without this oscillation, and therefore the initial oscillation is not responsible for the self-rotation
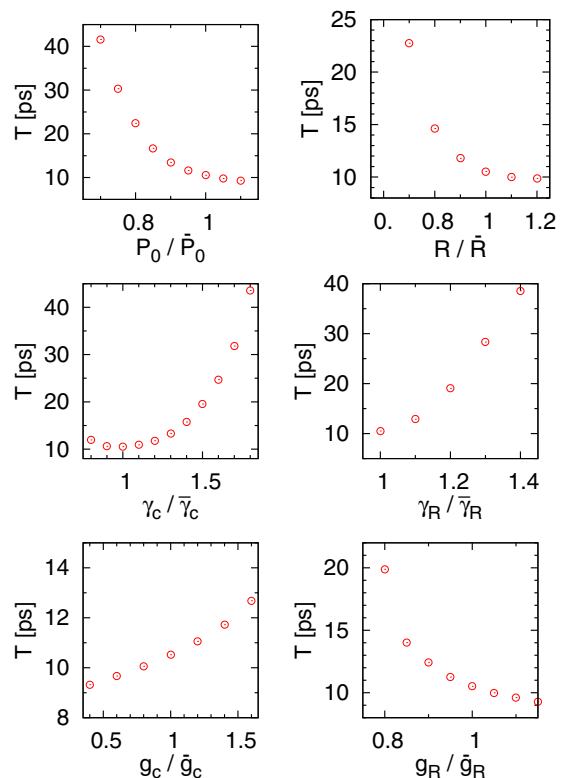

FIG. 3. Parameter dependence of the period T of the self-rotation. The parameters except for the abscissas are $\bar{P}_0 = 160$ ps^{-1} μm^{-2}, $\bar{R} = 0.04$ ps^{-1} μm^2, $\bar{\gamma}_c = 0.15$ ps, $\bar{\gamma}_R = 3$ ps, $\bar{g}_c = 6 \times 10^{-3}$ meV μm^2, and $\bar{g}_R = 2\bar{g}_c$.

(see Appendix). It may be better to use a dual reservoir model [25,31] to suppress the initial oscillation.

IV. SYNCHRONIZATION BETWEEN TWO ROTATING CONDENSATES

We study the case in which two self-rotating condensates are excited by two Gaussian laser beams, and examine whether synchronization occurs between the two self-rotations. The external pump is given by

$$P(\boldsymbol{r}) = P_{\text{left}}e^{-(\boldsymbol{r}-\boldsymbol{R}_{\text{left}})^2/\rho^2} + P_{\text{right}}e^{-(\boldsymbol{r}-\boldsymbol{R}_{\text{right}})^2/\rho^2}, \qquad (6)$$

where $P_{\text{left,right}}$ and $\boldsymbol{R}_{\text{left,right}} = (X_{\text{left,right}}, Y_{\text{left,right}})$ are the peak intensities and the positions of the two Gaussian-shaped pumps, respectively. Without loss of generality, we set $Y_{\text{left,right}} = 0$. The pump intensities are taken to be $P_{\text{left}} = 160$ ps^{-1} μm^{-2} and $P_{\text{right}} = 0.99 P_{\text{left}}$, which results in different self-rotation frequencies (see Fig. 3). If the two self-rotating condensates are independent (i.e., in the case of $X_{\text{right}} - X_{\text{left}} \to \infty$), then the rotation period is 10.52 ps for P_{left} and 10.70 ps for P_{right}. The c.m. position of each condensate is defined relative to the center of the pump as

$$\langle \boldsymbol{r} \rangle_{\text{left,right}} = \frac{\int_{|\boldsymbol{r}-\boldsymbol{R}_{\text{left,right}}|<r_c} (\boldsymbol{r} - \boldsymbol{R}_{\text{left,right}})|\psi|^2 d\boldsymbol{r}}{\int_{|\boldsymbol{r}-\boldsymbol{R}_{\text{left,right}}|<r_c} |\psi|^2 d\boldsymbol{r}}, \qquad (7)$$

where the cutoff radius r_c is taken to be 8 μm, which is sufficient to cover each condensate.
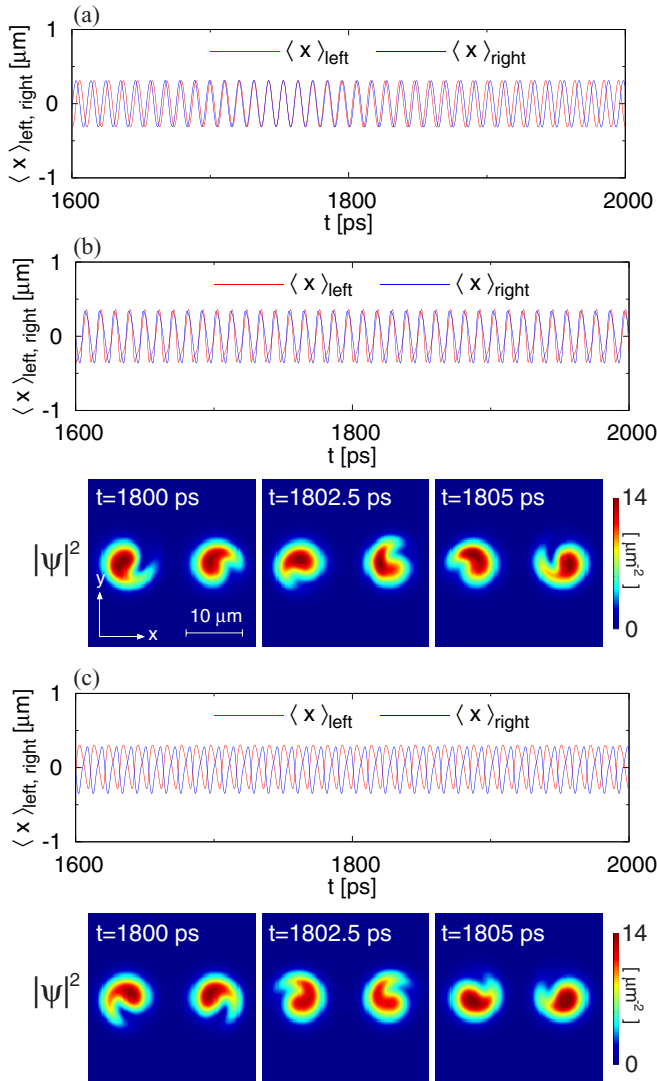
FIG. 4. Dynamics of two self-rotating condensates pumped according to Eq. (6) with $P_{\text{left}} = 160$ ps^{-1} μm^{-2}, $P_{\text{right}} = 0.99 P_{\text{left}}$, and $\rho = 5$ μm. The other parameters are $\gamma_c^{-1} = 0.15$ ps, $\gamma_R^{-1} = 3$ ps, $g_c = 6 \times 10^{-3}$ meV μm^2, $g_R = 2g_c$, and $R = 0.04$ ps^{-1} μm^2. (a) Time evolution of $\langle x \rangle_{\text{left}}$ and $\langle x \rangle_{\text{right}}$ with $X_{\text{right}} - X_{\text{left}} = 20$ μm. The two self-rotations are not synchronized. (b) Time evolution of $\langle x \rangle_{\text{left}}$ and $\langle x \rangle_{\text{right}}$ (upper panel) and snapshots of the density profile $|\psi|^2$ (lower panels), where $X_{\text{right}} - X_{\text{left}} = 16$ μm. Synchronization occurs between the two self-rotating condensates. (c) The same conditions as those in (b), except a random number seed used to produce the initial noise. See the Supplemental Material for movies of the dynamics in (b) and (c) [30].

Figure 4(a) shows the time evolution of the two self-rotating condensates, where the distance between the two pumps is $X_{\text{right}} - X_{\text{left}} = 20$ μm. In this case, the two condensates are well separated from each other and the interaction between them is negligible. The left- and right-side condensates rotate independently with periods of 10.52 and 10.70 ps, respectively, and no synchronization occurs. The self-rotation always occurs for both condensates irrespective of the random noise. Figure 4(b) shows the synchronization for $X_{\text{right}} - X_{\text{left}} = 16$ μm. The c.m. positions $\langle x \rangle_{\text{left}}$ and $\langle x \rangle_{\text{right}}$ oscillate in
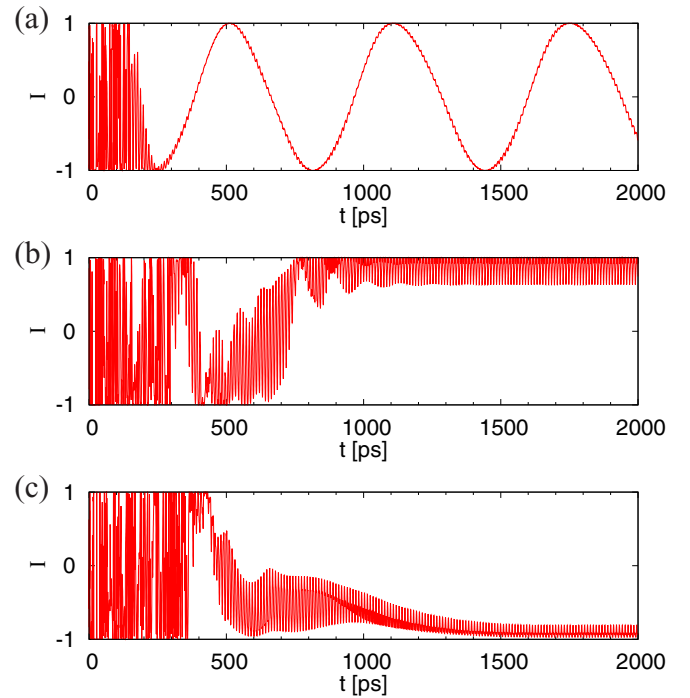

FIG. 5. Time evolution of I defined in Eq. (8), where (a)–(c) correspond to the dynamics shown in Figs. 4(a)–4(c).

phase at the same frequency. The two condensates rotate in opposite directions with a common rotation period of 10.53 ps, by which it seems that the right-side frequency is entrained into the left-side frequency [32]. Interestingly, another type of synchronization is observed for the same parameters, which is shown in Fig. 4(c). The c.m. positions $\langle x \rangle_{\text{left}}$ and $\langle x \rangle_{\text{right}}$ oscillate out of phase with a period of 10.55 ps. The only difference between the numerical simulations in Figs. 4(b) and 4(c) is the random number seed used to produce the small initial noise. We have also confirmed that the synchronization can occur for a sample with disorder [30].

To clearly visualize the synchronization, the inner product is calculated:

$$I = \hat{x}_{\text{left}} \hat{x}_{\text{right}} - \hat{y}_{\text{left}} \hat{y}_{\text{right}}, \qquad (8)$$

where $\hat{\boldsymbol{r}}_{\text{left,right}} = \langle \boldsymbol{r} \rangle_{\text{left,right}} / |\langle \boldsymbol{r} \rangle_{\text{left,right}}|$ are the unit vectors of the c.m. positions relative to the centers of the pumps. The minus sign in Eq. (8) is introduced to quantify the synchronization between the opposite rotations, as shown in Figs. 4(b) and 4(c). If the two unit vectors rotate in the opposite directions as $x_{\text{left}} + i y_{\text{left}} = e^{i\omega t}$ and $x_{\text{right}} + i y_{\text{right}} = e^{-i\omega' t + \phi}$, then $I = \cos[(\omega - \omega')t + \phi]$. When frequency lock occurs, I becomes constant.

Figures 5(a)–5(c) show the time evolution of I, which correspond to the dynamics shown in Figs. 4(a)–4(c), respectively. When the two self-rotations are not synchronized, I oscillates at their frequency difference, as shown in Fig. 5(a), where the period is $\simeq (10.52^{-1} - 10.7^{-1})^{-1} \simeq 625$ ps. When synchronization occurs, I oscillates around a constant value, as shown in Figs. 5(b) and 5(c). The synchronized phase ϕ is $\simeq 0$ in Fig. 5(b) and $\simeq \pi$ in Fig. 5(c).
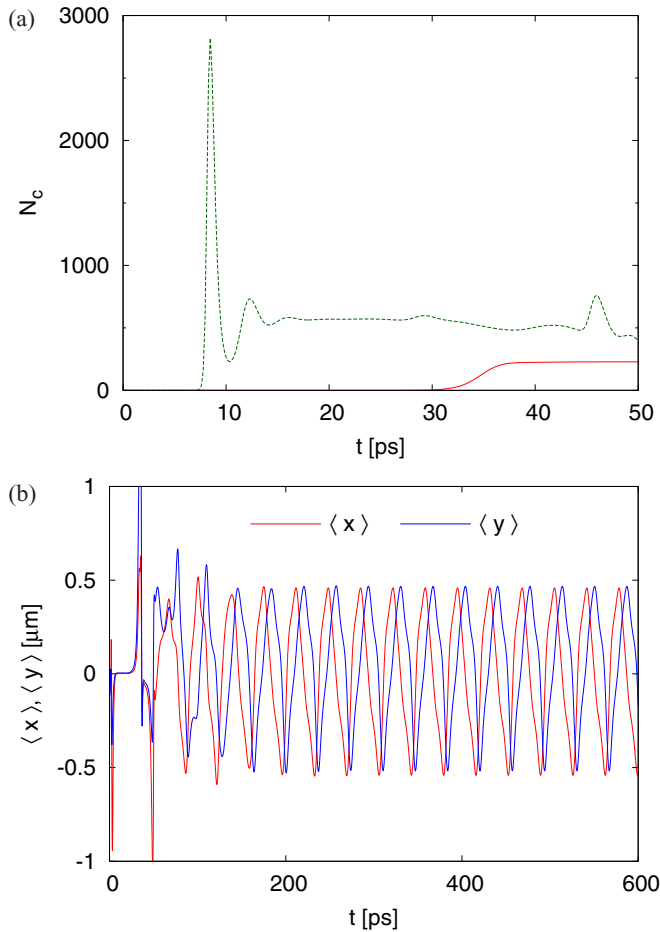
FIG. 6. Time evolution of (a) $N_c = \int |\psi|^2 d\boldsymbol{r}$ (solid curve) and (b) the c.m. position $(\langle x \rangle, \langle y \rangle)$ for $\gamma_c^{-1} = 0.19$ ps, $\gamma_R^{-1} = 0.86$ ps, $g_c = 3.6 \times 10^{-3}$ meV μm^2, $g_R = 17.3 g_c$, and $R = 0.04$ ps^{-1} μm^2, and $P_0 = 272$ ps^{-1} μm^{-2}, where $\rho = 4.5$ μm in (a) and $\rho = 5.6$ μm in (b). The dashed curve in (a) shows N_c for the same parameters as those in Fig. 2.

V. CONCLUSIONS AND DISCUSSION

We have investigated the dynamics of an exciton-polariton condensate in a planar semiconductor microcavity pumped by a nonresonant laser beam. We considered a parameter region in which modulational instability arises in a homogeneous system (Fig. 1). It was shown that when the polariton condensate is excited by a Gaussian laser beam of which the width

is comparable to the unstable wavelength, the self-rotation of the condensate occurs; the c.m. position of the condensate wave packet rotates around the center of the pump at a constant frequency (Fig. 2). The parameter dependence of the self-rotation frequency was investigated (Fig. 3). In addition, the synchronization of two self-rotating condensates pumped by two Gaussian laser beams was investigated (Figs. 4 and 5). The two self-rotations could be synchronized, even when the individual rotation frequencies were slightly different. We have also confirmed that the self-rotation and synchronization can be observed even in the presence of disorder potential in a realistic sample.

Spontaneous rotation has been studied for the nonlinear Schrödinger equation with pump and decay [33], and recently a wave packet of a condensate in a harmonic potential was found to rotate spontaneously [34]. The mechanism for these spontaneous rotations may be different from that presented here, because only the condensate wave function was considered in these previous studies, while the interplay between the condensate and the reservoir plays an important role in the self-rotation in this work.

APPENDIX: SELF-ROTATION WITH MODERATE CONDENSATE GROWTH

For the parameters used in Fig. 2, the present model exhibits unrealistic violent oscillation between the numbers of condensate and reservoir polaritons in the early stage of the dynamics. In this Appendix, we show that this oscillatory behavior is not responsible for the self-rotation.

Figure 6(a) shows the initial growth of the condensate polaritons $N_c = \int |\psi|^2 d\boldsymbol{r}$. For the same parameters as those in Fig. 2, N_c strongly oscillates at $t \sim 10$ ps (dashed curve). On the other hand, for a new parameter set with a shorter reservoir lifetime, the condensate grows smoothly (solid curve). Figure 6(b) shows the time evolution of the c.m. position for this parameter set, which exhibits self-rotation after $t \simeq 150$ ps. Thus, the self-rotation occurs even without the initial oscillation in N_c and therefore the initial oscillatory behavior is not responsible for the self-rotation.

[1] A. Jenkins, Phys. Rep. **525**, 167 (2013).

[2] C. Huygens, in *Oeuvres complétes de Christiaan Huygens*, edited by D. B. de Haan (Martinus Nijhoff, Den Haag, 1893), Vol. 5.

[3] T. Carmon, H. Rokhsari, L. Yang, T. J. Kippenberg, and K. J. Vahala, Phys. Rev. Lett. **94**, 223902 (2005).

[4] T. J. Kippenberg, H. Rokhsari, T. Carmon, A. Scherer, and K. J. Vahala, Phys. Rev. Lett. **95**, 033901 (2005).

[5] D. A. Rodrigues, J. Imbers, and A. D. Armour, Phys. Rev. Lett. **98**, 067204 (2007).

[6] I. Carusotto and C. Ciuti, Rev. Mod. Phys. **85**, 299 (2013).

[7] T. Byrnes, N. Y. Kim, and Y. Yamamoto, Nat. Phys. **10**, 803 (2014).

[8] J. Kasprzak, M. Richard, S. Kundermann, A. Baas, P. Jeambrun, J. M. J. Keeling, F. M. Marchetti, M. H. Szymańska, R. André, J. L. Staehli, V. Savona, P. B. Littlewood, B. Deveaud, and Le Si Dang, Nature (London) **443**, 409 (2006).

[9] K. G. Lagoudakis, M. Wouters, M. Richard, A. Baas, I. Carusotto, R. André, Le Si Dang, and B. Deveaut-Plédran, Nat. Phys. **4**, 706 (2008).

[10] G. Roumpos, M. D. Fraser, A. Löffler, S. Höfling, A. Forchel, and Y. Yamamoto, Nat. Phys. **7**, 129 (2011).

[11] A. Amo, D. Sanvitto, F. P. Laussy, D. Ballarini, E. del Valle, M. D. Martin, A. Lemaître, J. Bloch, D. N. Krizhanovskii, M. S. Skolnick, C. Tejedor, and L. Viña, Nature (London) **457**, 291 (2009).

[12] G. Nardin, G. Grosso, Y. Léger, B. Pietka, F. Morier-Genoud, and B. Deveaut-Plédran, Nat. Phys. **7**, 635 (2011).

[13] A. Amo, S. Pigeon, D. Sanvitto, V. G. Sala, R. Hivet, I. Carusotto, F. Pisanello, G. Leménager, R. Houdré, E. Giacobino, C. Ciuti, and A. Bramati, Science **332**, 1167 (2011).

[14] G. Grosso, G. Nardin, F. Morier-Genoud, Y. Léger, and B. Deveaud-Plédran, Phys. Rev. Lett. **107**, 245301 (2011).

[15] T. Gao, E. Estrecho, K. Y. Bliokh, T. C. H. Liew, M. D. Fraser, S. Brodbeck, M. Kamp, C. Schneider, S. Höfling, Y. Yamamoto, F. Nori, Y. S. Kivshar, A. G. Truscott, R. G. Dall, and E. A. Ostrovskaya, Nature (London) **526**, 554 (2015).

[16] M. Wouters, Phys. Rev. B **77**, 121302(R) (2008).

[17] P. R. Eastham, Phys. Rev. B **78**, 035319 (2008).

[18] M. O. Borgh, J. Keeling, and N. G. Berloff, Phys. Rev. B **81**, 235302 (2010).

[19] D. Read, Y. G. Rubo, and A. V. Kavokin, Phys. Rev. B **81**, 235315 (2010).

[20] N. Bobrovska, E. A. Ostrovskaya, and M. Matuszewski, Phys. Rev. B **90**, 205304 (2014).

[21] K. Rayanov, B. L. Altshuler, Y. G. Rubo, and S. Flach, Phys. Rev. Lett. **114**, 193901 (2015).

[22] X. Ma, I. Yu. Chestnov, M. V. Charukhchyan, A. P. Alodjants, and O. A. Egorov, Phys. Rev. B **91**, 214301 (2015).

[23] T.-W. Chen, S.-D. Jheng, W.-F. Hsieh, and S.-C. Cheng, Superlattices Microstruct. **92**, 190 (2016).

[24] A. Baas, K. G. Lagoudakis, M. Richard, R. André, Le Si Dang, and B. Deveaud-Plédran, Phys. Rev. Lett. **100**, 170401 (2008).

[25] K. G. Lagoudakis, B. Pietka, M. Wouters, R. André, and B. Deveaud-Plédran, Phys. Rev. Lett. **105**, 120403 (2010).

[26] H. Saito, T. Aioi, and T. Kadokura, Phys. Rev. B **86**, 014504 (2012).

[27] M. Wouters and I. Carusotto, Phys. Rev. Lett. **99**, 140402 (2007).

[28] L. A. Smirnov, D. A. Smirnova, E. A. Ostrovskaya, and Y. S. Kivshar, Phys. Rev. B **89**, 235310 (2014).

[29] T. C. H. Liew, O. A. Egorov, M. Matuszewski, O. Kyriienko, X. Ma, and E. A. Ostrovskaya, Phys. Rev. B **91**, 085413 (2015).

[30] See Supplemental Material at http://link.aps.org/supplemental/10.1103/PhysRevB.94.165306 for movies of the condensate and reservoir dynamics.

[31] G. Nardin, K. G. Lagoudakis, M. Wouters, M. Richard, A. Baas, R. André, Le Si Dang, B. Pietka, and B. Deveaud-Plédran, Phys. Rev. Lett. **103**, 256402 (2009).

[32] A. Pikovsky, M. Rosenblum, and J. Kurths, *Synchronization: A Universal Concept in Nonlinear Sciences* (Cambridge University Press, Cambridge, 2001).

[33] J. Keeling and N. G. Berloff, Phys. Rev. Lett. **100**, 250401 (2008).

[34] O. L. Berman, R. Ya. Kezerashvili, G. V. Kolmakov, and L. M. Pomirchi, Phys. Rev. E **91**, 062901 (2015).